Inkjet printed polymeric electron blocking and surface energy modifying layer for low dark current organic photodetectors

Andrea Grimoldi [a, b], Letizia Colella [a, c, 1], Lorenzo La Monaca [a, b], Giovanni Azzellino [a, b, 2], Mario Caironi [a, **], Chiara Bertarelli [a, c], Dario Natali [a, b, *], Marco Sampietro [a, b]

[a] Center for Nano Science and Technology@PoliMi, Istituto Italiano di Tecnologia, Via Giovanni Pascoli 70/3, 20133 Milano, Italy
[b] Dipartimento di Elettronica, Informazione e Bioingegneria Politecnico di Milano, Piazza Leonardo Da Vinci 32, 20133 Milano, Italy
[c] Dipartimento di Chimica, Materiali e Ingegneria Chimica "G. Natta", Politecnico di Milano, Piazza Leonardo da Vinci 32, 20133 Milano, Italy

[*] Corresponding author.
[**] Corresponding author.

E-mail addresses: mario.caironi@iit.it (M. Caironi), dario.natali@polimi.it (D. Natali)
1 INAFeOsservatorio Astronomico di Brera, via Bianchi 46, 23807, Merate, Italy
2 Research Laboratory of Electronics, Massachusetts Institute of Technology, 77 Massachusetts Avenue, Cambridge, MA 02139, USA

Abstract

The reduction of dark current is required to enhance the signal-to-noise ratio and decrease the power consumption in photodetectors. This is typically achieved by introducing additional functional layers to suppress carrier injection, a task that proves to be challenging especially in printed devices. Here we report on the successful reduction of dark current below 100 nA cm^{-2} (at -1 V bias) in an inkjet printed photodetector by the insertion of an electron blocking layer based on poly[3-(3,5-di-tert-butyl-4- methoxyphenyl)-thiophene], while preserving a high quantum yield. Furthermore, the electron blocking layer strongly increases the surface energy of the hydrophobic photoactive layer, therefore simplifying the printing of transparent top electrodes from water based formulations without the addition of surfactants.

1. Introduction

Nowadays photodetectors are used in many electronic systems ranging from telecommunications, imaging and security fields. In particular, emerging wearable and disposable applications require low cost manufacturing, large area fabrication, mechanical flexibility and lightweight which are features hard to be obtained with silicon technology. Additive, cost-effective, scalable printing techniques (e.g. roll-to-roll, inkjet printing, screen printing, spray coating) are perfectly suitable for the development of large-area, distributed, complex optoelectronic systems [1,2]. Among printing technologies, inkjet offers the capability of transferring a digital pattern directly and without contact on a variety of substrates and it is an easily customizable technique [3]. In order to develop printed devices that cope with the aforementioned needs, functional inks of organic materials are good candidates, thanks to their peculiar features such as solution processability, chemically tailorable properties, abundance of primary materials, mechanical flexibility [4].
In the field of light sensing, some examples of printed photo- detectors have been already reported [5-8], yet the constraints related to the inkjet printing manufacturing resulted in some issues and/or in a trade-off between device complexity and device performances. Indeed, in addition to the photoactive layer and to the charge collecting electrodes, a photodetector ideally requires additional layers e termed hole and electron blocking

layers (HBL and EBL) e in order to suppress the injection of dark current, which otherwise limits the minimum detectable signal and increases power consumption [9-17]. The development of printable HBLs and EBLs is a non-trivial task, because each ink has to be tailored with proper rheological characteristics, and come from an orthogonal solvent respect to the underlying layer, in order to wet but not to dissolve/damage this latter.
In this work, we exploit a polythiophene derivative to develop an EBL that both reduces the dark current and strongly increases the surface energy of the hydrophobic photoactive layer used. As a result of the introduction of such EBL, we demonstrate a reduction of the dark current density below 100 nA cm^{-2} while preserving high quantum efficiency above 65%. Moreover, thanks to the increased surface energy, the top anode contact can be directly printed from a water-based poly(3,4-ethylenedioxythiophene):poly(styrenesulfonate) (PEDOT:PSS) formulation. This is advantageous because PEDOT:PSS water-based inks poorly wet the usually hydrophobic underlying photoactive layer. To overcome this issue a surfactant is often added [18], even in high amount [5], but this complicates the ink formulation; in addition the surfactant effects on PEDOT:PSS electronic and mechanical properties and ultimately on the device performance are still poorly understood [19]. Other possible strategies are the insertion of a self-assembled monolayer or plasma treatment of the photoactive blend. The possibility of tuning the surface energy simply by printing this EBL makes the fabrication process more suitable for industrialization.

2. Materials and methods

Reference samples were prepared similarly to the ones reported in Ref. [5]: polyethylenenaphthalate (PEN) (DuPont) was used as substrate, silver TEC-IJ 060 (InkTec) ink was printed with Dimatix DMP2831 with 10 pl nozzle and sintered in air at 140 oC to realize aligning reference marks and easy contactable electrical probe points. Clevios P Jet 700 N (Hereaus) PEDOT:PSS ink was filtered with 0.2 mm PVDF filter and printed with DMP2831 10 pl cartridge. The HBL was realized using branched polyethylenimine (PEI) (Sigma Aldrich) diluted in 2-methoxyethanol (0.1 wt% concentration) and spin-coated over the bottom contacts at 5000 rpm (1000 rpm/s) for 1min. Poly(3-hexylthiophene) (P3HT) (RR ¼ 96.6%, MW ¼ 65500) was purchased from Merck, and [6,6]- phenyl-C61 butyric acid methyl ester (PCBM) (purity > 99.5%) was purchased from Solenne. Both were used as received. P3HT:PCBM (1:1) blend was dissolved in 1,2-dichlorobenzene (68 vol%) and mesitylene (32 vol%) solution and stirred overnight. The blend solution was heated at 80 ^{o}C for 10 min, filtered with a 0.20 mm PTFE filter and inkjet printed with a Microfab JETLAB 4 equipped with a 40 mm diameter DLC nozzle. Clevios P Jet 700 N was printed over the blend with Zonyl FS-300 fluorosurfactant (Sigma Aldrich) added to the fluid (10 wt%).
For the EBL poly[3-(3,5-di-tert-butyl-4-methoxyphenyl)-thiophene] (poly-PT) [20] was synthesized according to the procedure reported in the Supporting Information. Poly-PT was characterized through Bruker NMR ARX400. For the fabrication of devices with EBL, 4 mg of poly-PT, extracted with n-hexane, were dissolved in1 ml of n-butanol:ethylene glycol (9:1) and heated at 70 ^{o}C for 1 h. The ink was heated at 80 ^{o}C for 10 min before use and filtered with a 1.45μm PVDF filter. Poly-PT was printed on P3HT:PCBM by means of a DMP2831 inkjet printer equipped with 10 pl nozzles on top of the active blend or spin-coated in three steps (200 rpm, 100 rpm/s, 6 s; 1000 rpm, 200 rpm/s, 80 s; 5000 rpm, 1000 rpm/s, 60 s). On top of poly-PT, Clevios P Jet 700 N was printed with or without Zonyl FS-300. We realized the following device configurations by keeping the bottommost layers fixed, viz. PEDOT:PSS/PEI/P3HT:PCBM and changing the topmost ones (Fig. 1B):

(a) ../poly-PT spin-coated/PEDOT:PSS
(b) ../poly-PT printed/PEDOT:PSS þ Zonyl
(c) ../poly-PT spin-coated/PEDOT:PSS þ Zonyl
(d) ../PEDOT:PSS þ Zonyl
(e) ../n-butanol:ethylene glycol/PEDOT:PSS þ Zonyl

The entire fabrication process was carried out in ambient condition. Profiles were measured by stylus profilometry (KLA Tencor Alpha-Step IQ, minimum detectable thickness 5 nm). A Varian Cary 50 Spectrophotometer was used to measure layer absorbance.
Contact angles were measured using a Dataphysics OCA 15EC. We define the bias voltage as the potential difference between the top and the bottom electrode. Current-Voltage (I-V) measurements were recorded in a nitrogen-filled glove box in dark and under white light (6400 K, about 3 mW cm^{-2}) on nine devices. External Quantum Efficiency (EQE) spectra were recorded at about 1 mW cm^{-2} in glovebox. EQE spectra and power dependences were taken with the device under test biased at -1V.

3. Results and discussion

The poly-PT was chemically engineered to act as an EBL for a P3HT:PCBM blend based photodetector in the device configuration showed in Fig. 1. On the one hand the presence of the bulky 3,5-di- tert-butyl-4-methoxyphenyl induces distortion of the backbone, thus leading to a short conjugation length (i.e. large energy gap) and a LUMO level (lowest unoccupied molecular orbital) at -2.3 eV; on the other hand the HOMO level (highest occupied molecular orbital) is located at -5.0 eV, in order to allow efficient holes collection from P3HT.
The raw poly-PT was precipitated from methanol and was fractioned by hot extraction with two different solvents (i.e. n- hexane and chloroform). The fraction of poly-PT recovered from n- hexane was chosen as it was soluble in many organic solvents. A proper solvent choice allowed the formulation of a printable ink orthogonal to the P3HT:PCBM-based blend (see Supplementary Information for more details). Different classes of solvents have been tested to assess possible dissolution or modification of the P3HT:PCBM layer. N-alkanes and ethers led to a decrease of the photoactive layer thickness, whereas alcohols have demonstrated to be a convenient choice. Among these, isopropanol and hexanol were ruled out for the device fabrication because the low boiling point of the former led to nozzle clogging related to fast solvent evaporation at the orifice, while the high boiling point of the latter left the deposited layer wet even after two hours at room temperature. These two issues were overcome using n-butanol as main solvent and obtaining an ink with boiling point in between the isopropanol and the hexanol ones.

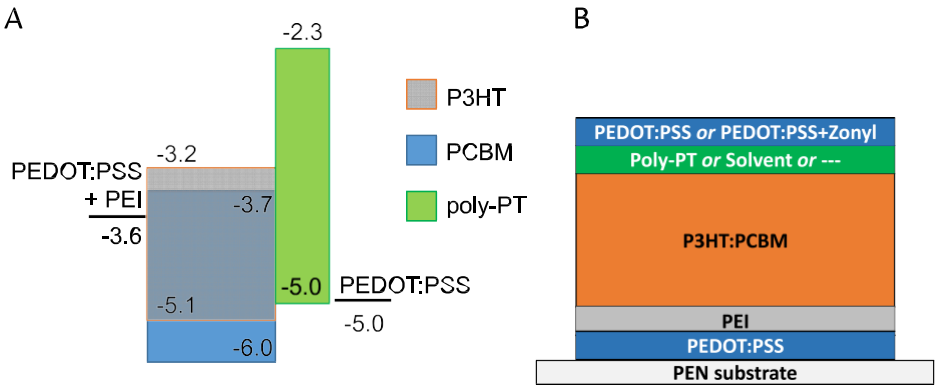

Fig.1. Energy levels scheme (A) and structure of the device (B). PEI functionalized PEDOT:PSS work function was taken from Ref. [10].

The devices were fabricated in a vertical structure with an about 100 nm thick photoactive blend sandwiched in between two printed PEDOT:PSS-based electrodes. Both the top and bottom electrodes are transparent, making possible to impinge with light from both sides [7]. In this work devices were tested by shining light from the top side. The active area resulting by the overlapping of bottom and top electrodes is about 100 mm x 80 mm. HBL (EBL) was placed between the bottom (top) electrode and the photo- active material. A

reference sample, namely (d), fabricated according to such architecture without the presence of the EBL, shows an EQE peak of 73% at 470-505 nm (Fig. 2A). The same device displays a dark current density with an average value of 200 nA cm^{-2} (best device: 130 nA cm^{-2}) (Fig. 2B). Assuming the dark current shot noise as the dominant noise component, the peak specific detectivity (D*) results to be 1.45 x 10^{12} Jones under 505 nm light (neglecting the 1/f component may result in an overestimation of D*). EQE and dark current density of these detectors are comparable with the previously reported examples of printed photodetectors and among the best P3HT:PCBM based detectors irrespective of the fabrication technique [5,21-24].
Firstly, we investigated the role of the additional layer of poly- PT, either printed or spin-coated, comparing devices (b) and (c) to the reference (d) keeping constant the recipe for the other layers, e.g. fluorosurfactant is added to top electrode ink of the three de- vice kinds. For all (b), (c) and (d) devices EQE spectra show values in excess of 65% between 450 nm and 525 nm and no significant difference in spectral shape (Fig. 2A). This indicates that poly-PT: i) does not sizably affect light absorption, in agreement with its high transmittance in the visible range; ii) does not hinder hole collection, being its HOMO well aligned with P3HT HOMO. In Fig. 2B statistical data on dark current density are reported: when the EBL is present, either spin-coated or printed, dark current density is reduced more than twice reaching a mean value of 75 nA cm^{-2} (best device: 55 nA cm-2), with -1V bias applied. Calculated peak specific detectivity (D*) results to be 2.2 x 10^{12} Jones for (b) and (c) at 505 nm light which is 1.5 times higher than the reference (d). We would like to stress out that poly-PT improves D* also when it is inkjet printed, allowing the fabrication of an all-printed device. Devices with poly-PT show limited (<100 nA cm^{-2}) dark current for bias as low as -1.5 V (Fig. S8).

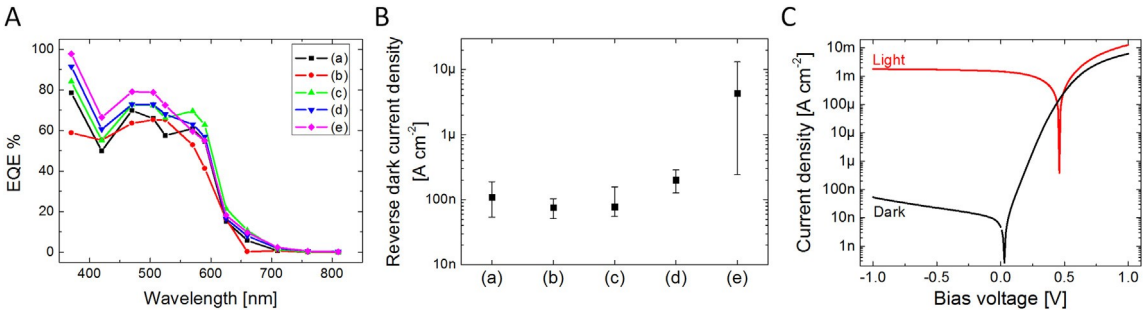

Fig. 2. (A) EQE spectra of devices (a), (b), (c), (d) and (e) biased at -1V. (B) Dark current density statistics for fabricated devices measured with a bias of -1V. Bars indicate maximum and minimum measured values. (C) I-V characteristics are reported of the best (a) device in dark (continuous line) and under 3 mW cm^{-2} 6400 K white light (dashed line).

In order to discriminate the effect of poly-PT solvent alone from the one of the polymer itself we realized devices (e) by spin-coating n-butanol:ethylene glycol (9:1) instead of the poly-PT solution, setting the same spin-coating parameters used for EBL deposition. These devices exhibit a dramatic increase of the dark current density mean value and dispersion: these observations highlight that the positive effect on dark current density is due only to the electron blocking polymer and is not related to solvent effect [25-29].
We have completed the electrical characterization of the aforementioned devices by measuring their response time, extracted as the 90%-10% photocurrent fall time upon the application of a 1.7 mW cm^{-2} light pulse (Table 1). The response time is 106 ms both for reference (d) and solvent-only (e) devices. When poly-PT is inkjet printed (b), the response time gets mildly higher (136 ms), whereas when poly-PT is spun (c) the response time is more than twice as large with respect to the reference (d). The choice of printing the EBL instead of relying on spin-coating has thus the advantage of improving the detectivity while moderately affecting the device speed.

Table 1 – Figures of merit of the different devices kinds.

Device PEDOT:PSS/PEI/P3HT:PCBM/..	Reverse dark current density (mean value) [nA cm^{-2}]	Forward dark current density (mean value) [mA cm^{-2}]	Peak EQE %	Response time [ms]	Bare P JET 700 N adhesion
(a) ../poly-PT spin-coated /PEDOT:PSS	108.2	2.0	70	451	Yes
(b) ../poly-PT printed /PEDOT:PSS + Zonyl	75.8	8.7	65	136	Yes
(c) ../poly-PT spin-coated /PEDOT:PSS + Zonyl	77.7	4.7	73	254	Yes
(d) ../PEDOT:PSS + Zonyl	200.9	48.8	73	106	No
(e) ../*n*-butanol:ethylene glycol /PEDOT:PSS + Zonyl	4327.8	42.8	79	106	No

Devices (c) show response time independent of the applied bias (Fig. 3A). This evidence rules out the transit time as the main limitation to device speed and suggests that these devices operate in a photoconductive regime [30], where moving carriers circulate e being collected and re-injected e until they recombine with slow carriers of the opposite sign, the probability of this event being unaffected (to a first degree) by the electric field. In P3HT:PCBM blends electrons, which have a larger mobility than holes, are expected to play the role of moving carriers and holes the role of slow carriers [31]. The photoconductive regime is indeed confirmed not only for (c) but also for all the other kinds of photodetectors (Fig. S3) because in all cases EQE is above unity at low light intensity [32]. As to the slower response time of (b) and (c) compared to (d), we observe that solvent-treated devices (d) exhibit the same response time of reference devices (e), hence solvent-induced modification to the bulk can be excluded and the lower speed has to be traced back to poly-PT itself, and/or to one or both the interfaces blend/poly-PT and polyPT/PEDOT:PSS. As a tentative explanation, we can hypothesize that when poly-PT is present, additional trapping states for holes with a relatively slow temporal dynamics are created. The correlation between defects in anodic interlayers and organic photodiode temporal response has been underlined in a recent work [33]. The difference in response speed of devices (b) and (c) could possibly be related to differences in the morphology and/or in the interface energetics of the printed poly- PT layer compared to the spin-coated one [34].

I-V curves of device (c) exhibit a forward dark current density of 40 mA cm^{-2} in average at +1 V (Fig. 3B), which is the same as the reference (d) and ranging among the best P3HT:PCBM based detectors [24,35]. Instead, the forward current density of detector (b) in dark is almost one order of magnitude lower. The worse hole injection through the printed poly-PT is likely related to a different thickness or morphology of the printed EBL compared to the spin- coated one [34].

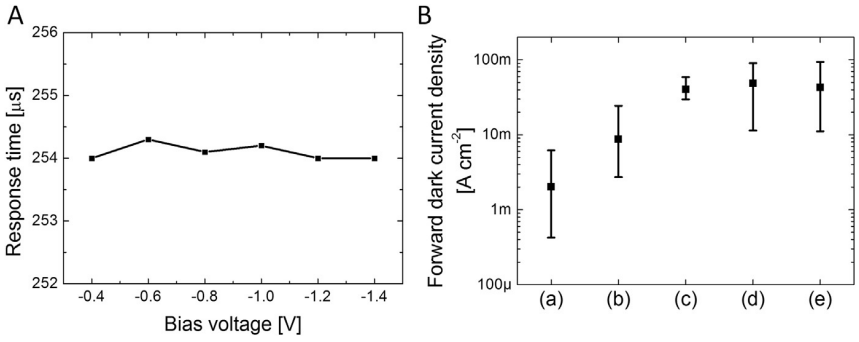

Fig. 3. (A) Response time measured on device (c) at different bias voltages (impinging light 570 nm, 1.7 mW cm^{-2}). (B) Dark current density statistics for fabricated devices measured with a bias of +1V. Bars indicate maximum and minimum measured values.

Finally, we verified that the presence of poly-PT simplifies the deposition of the top anode thanks to its superior wettability with respect to bare P3HT:PCBM blend. Optical micrographs show that Zonyl addition is mandatory to realize a continuous top electrode for photodetectors realized without poly-PT (Fig. 4A and B), while with poly-PT a continuous top PEDOT:PSS contact can be obtained even without the Zonyl addition (Fig. 4C). Fig. 4D and E show the side view of 1 ml P JET 700 N droplet dispensed on bare P3HT:PCBM and on the stack P3HT:PCBM/poly-PT. The contact angle is 16° in presence of the EBL while it is 36o without it, demonstrating that bare P JET 700 N can be printed more easily on poly-PT than on P3HT:PCBM. We verified that poly-PT solvent (n-butanol:ethylene glycol (9:1)) alone is not effective in modifying the wettability (see Supplementary Information for more details). We point out that there is no significant difference between samples (c) with, and (a) without Zonyl in terms of EQE (Fig. 2A), reverse dark currents (Fig. 2B) and response time (Fig. S4A). Conversely, the absence of Zonyl affects the forward current density that is reduced by a factor 10.

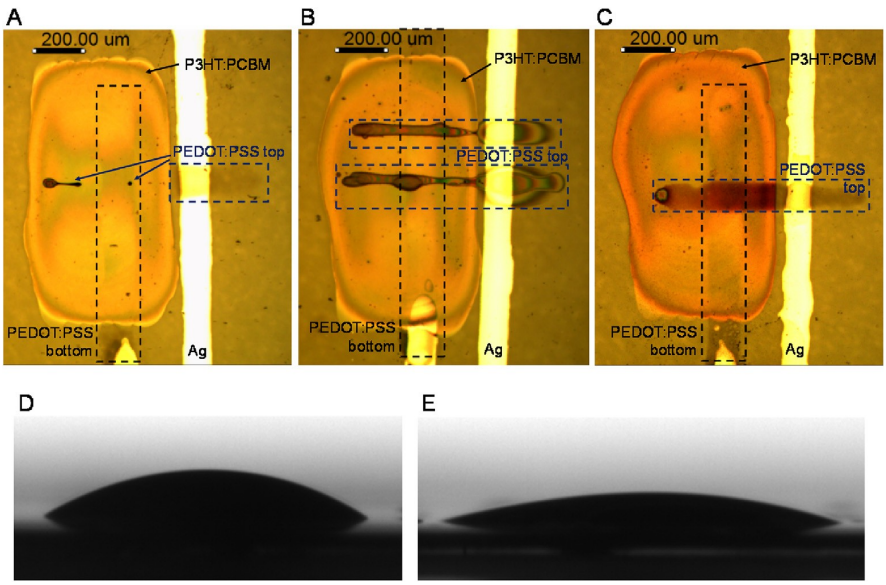

Fig. 4. Optical micrographs of photodetectors realized without poly-PT nor Zonyl addition (A), without poly-PT with Zonyl addition (B), with poly-PT without Zonyl addition (C). Scale bar 200 mm. Dashed lines highlight PEDOT:PSS bottom (black) and top (blue) contacts. PEDOT:PSS droplet on bare P3HT:PCBM (D) and on P3HT:PCBM/poly-PT (E). Contact angles are of 35° and 16°, respectively. For contact angle measurements P3HT:PCBM was spin-coated on PEN at 1000 rpm, 500 rpm s^{-1}, for 60 s. Results for the different devices are summarized in Table 1. (For interpretation of the references to colour in this figure legend, the reader is referred to the web version of this article.)

These results lead to the hypothesis that different top electrode adhesion is the cause for a worse injection of holes from top contact. Shelf life was measured for a device with printed poly-PT (b) kept in the dark and in nitrogen atmosphere inside a glovebox. I-V curves were measured after 15 months from device fabrication (Fig. S7). Forward current density and open circuit voltage of the device result lowered compared to the fresh device. On the other hand, not only the photocurrent remains unchanged, but reverse dark current density is reduced reaching the value of 34 nA cm^{-2}. The light to dark ratio results more than doubled with respect to the first measurement.

4. Conclusions

Thanks to the insertion of poly-PT as an electron blocking layer and the consequent increase in surface energy, it was possible to fabricate fully-organic, inkjet printed photodetectors where the top anode electrode could be simply processed from a PEDOT:PSS formulation without the addition of a fluorosurfactant. Importantly, the insertion of the printed EBL succeeded in halving average dark current densities, resulting in 75 nA cm^{-2}, while maintaining EQE as high as 65%. The addition of the printed poly-PT layer mildly affects the device response time, which turns out to be of 136 ms. These achievements on printed, semitransparent photodetectors with low dark currents can pave the way for a cost-effective integration of this sensing element in interactive surfaces and imaging systems with challenging SNR requirements such as medical imaging, biosensing and night vision.

Acknowledgments

Fondazione Cariplo is acknowledged for financial support through the InDiXi project grant n. 2011e0368. M. C. acknowledges partial financial support from European Union through the Marie- Curie Career Integration Grant 2011 “IPPIA”, within the EU Seventh Framework Programme (FP7/2007-2013) under grant agreement No. PCIG09-GA-2011-291844.

References

[1] K.J. Baeg, M. Caironi, Y.Y. Noh, Toward printed integrated circuits based on unipolar or ambipolar polymer semiconductors, Adv. Mater. 25 (2013) 4210-4244, http://dx.doi.org/10.1002/adma.201205361.

[2] G. Dell’Erba, A. Perinot, A. Grimoldi, D. Natali, M. Caironi, Fully-Printed, all- polymer integrated twilight switch, Semicond. Sci. Technol. 30 (2015) 104005, http://dx.doi.org/10.1088/0268-1242/30/10/104005.

[3] B.-J. de Gans, L. Xue, U.S. Agarwal, U.S. Schubert, Ink-Jet printing of linear and star polymers, Macromol. Rapid Commun. 26 (2005) 310e314, http://dx.doi.org/10.1002/marc.200400503.

[4] H. Marien, M. Steyaert, P. Heremans, Analog Organic Electronics, Analog Circuits Signal Process, 2013, pp. 1e13, http://dx.doi.org/10.1007/978-1-4614- 3421-4.

[5] G. Azzellino, a. Grimoldi, M. Binda, M. Caironi, D. Natali, M. Sampietro, Fully inkjet-printed organic photodetectors with high quantum yield, Adv. Mater. 25 (2013) 6829-6833, http://dx.doi.org/10.1002/adma.201303473.

[6] G. Pace, A. Grimoldi, M. Sampietro, D. Natali, M. Caironi, Printed photodetectors, Semicond. Sci. Technol. 30 (2015) 104006, http://dx.doi.org/10.1088/ 0268-1242/30/10/104006.

[7] G. Pace, A. Grimoldi, D. Natali, M. Sampietro, J.E. Coughlin, G.C. Bazan, et al., All-organic and fully-printed semitransparent photodetectors based on nar- row bandgap conjugated molecules, Adv. Mater. 26 (2014) 6773-6777, http://dx.doi.org/10.1002/adma.201402918.

[8] A. Pierre, I. Deckman, P.B. Lechene, A.C. Arias, High detectivity all-printed organic photodiodes, Adv. Mater. 27 (2015) 6411-6417, http://dx.doi.org/ 10.1002/adma.201502238.

[9] K.-J. Baeg, M. Binda, D. Natali, M. Caironi, Y.-Y. Noh, Organic light detectors: photodiodes and phototransistors, Adv. Mater. 25 (2013) 4267-4295, http:// dx.doi.org/10.1002/adma.201204979.

[10] Y. Zhou, C. Fuentes-Hernandez, J. Shim, J. Meyer, A.J. Giordano, H. Li, et al., A universal method to produce low-work function electrodes for organic electronics, Science 336 (2012) 327-332, http://dx.doi.org/10.1126/ science.1218829.

[11] E. Saracco, B. Bouthinon, J.-M. Verilhac, C. Celle, N. Chevalier, D. Mariolle, et al., Work function tuning for high-performance solution-processed organic photodetectors with inverted structure, Adv. Mater. 25 (2013) 6534-6538, http://dx.doi.org/10.1002/adma.201302338.

[12] P.E. Keivanidis, S.H. Khong, P.K.H. Ho, N.C. Greenham, R.H. Friend, All-solution based device engineering of multilayer polymeric photodiodes: minimizing dark current, Appl. Phys. Lett. 94 (2009) 39-41, http://dx.doi.org/10.1063/ 1.3120547.

[13] M. Binda, A. Iacchetti, D. Natali, L. Beverina, M. Sassi, M. Sampietro, High detectivity squaraine-based near infrared photodetector with nA/cm[sup 2] dark current, Appl. Phys. Lett. 98 (2011) 073303, http://dx.doi.org/10.1063/1.3553767.

[14] M. Kaltenbrunner, T. Sekitani, J. Reeder, T. Yokota, K. Kuribara, T. Tokuhara, et al., An ultra-lightweight design for imperceptible plastic electronics, Nature 499 (2013) 458-463, http://dx.doi.org/10.1038/nature12314.

[15] J.R. Manders, T.-H. Lai, Y. An, W. Xu, J. Lee, D.Y. Kim, et al., Low-noise multi- spectral photodetectors made from all solution-processed inorganic semi- conductors, Adv. Funct. Mater. 24 (2014) 7205-7210, http://dx.doi.org/ 10.1002/adfm.201402094.

[16] S. Valouch, C. Hones, S.W. Kettlitz, N. Christ, H. Do, M.F.G. Klein, et al., Solution processed small molecule organic interfacial layers for low dark current polymer photodiodes, Org. Electron 13 (2012) 2727-2732, http://dx.doi.org/ 10.1016/j.orgel.2012.07.044.

[17] X. Gong, M. Tong, Y. Xia, W. Cai, J.S. Moon, Y. Cao, et al., High-detectivity polymer photodetectors with spectral response from 300 nm to 1450 nm, Science 325 (2009) 1665-1667, http://dx.doi.org/10.1126/science.1176706.

[18] L.L. Lavery, G.L. Whiting, A.C. Arias, All ink-jet printed polyfluorene photo- sensor for high illuminance detection, Org. Electron 12 (2011) 682e685, http://dx.doi.org/10.1016/j.orgel.2011.01.023.

[19] S. Jung, A. Sou, K. Banger, D.-H. Ko, P.C.Y. Chow, C.R. McNeill, et al., All-inkjet- printed, all-air-processed solar cells, Adv. Energy Mater. 3 (2014) 1400432, http://dx.doi.org/10.1002/aenm.201400432.

[20] T. Yamamoto, H. Hayashi, pi-Conjugated soluble and fluorescent poly (thiophene-2,5-diyl)s with phenolic, hindered phenolic and p-C6H4OCH3 Substituents. Preparation, optical properties, and redox reaction, J. Polym. Sci. Part A 35 (1997) 463-474, http://dx.doi.org/10.1002/(SICI)1099-0518(199702)35: 3<463::AID-POLA9>3.0.CO;2-T.

[21] M. Schmidt, A. Falco, M. Loch, P. Lugli, G. Scarpa, Spray coated indium-tin- oxide-free organic photodiodes with PEDOT: PSS anodes, AIP Adv. 4 (2014) 107132, http://dx.doi.org/10.1063/1.4899044.

[22] X. Liu, H. Wang, T. Yang, W. Zhang, X. Gong, Solution-processed ultrasensitive polymer photodetectors with high external quantum efficiency and detectivity, ACS Appl. Mater. Interfaces 4 (2012) 3701e3705, http://dx.doi.org/ 10.1021/am300787m.

[23] M. Ramuz, L. Bürgi, C. Winnewisser, P. Seitz, High sensitivity organic photo- diodes with low dark currents and increased lifetimes, Org. Electron 9 (2008) 369-376, http://dx.doi.org/10.1016/j.orgel.2008.01.007.

[24] C.N. Hoth, S. a. Choulis, P. Schilinsky, C.J. Brabec, On the effect of poly(3- hexylthiophene) regioregularity on inkjet printed organic solar cells, J. Mater. Chem. 19 (2009) 5398, http://dx.doi.org/10.1039/b823495g.

[25] H. Zhou, Y. Zhang, J. Seifter, S.D. Collins, C. Luo, G.C. Bazan, et al., High-efficiency polymer solar cells enhanced by solvent treatment, Adv. Mater. 25 (2013) 1646-1652, http://dx.doi.org/10.1002/adma.201204306.

[26] J.H. Seo, A. Gutacker, Y. Sun, H. Wu, F. Huang, Y. Cao, et al., Improved high- efficiency organic solar cells via incorporation of a conjugated poly- electrolyte interlayer, J. Am. Chem. Soc. 133 (2011) 8416-8419, http:// dx.doi.org/10.1021/ja2037673.

[27] X. Liu, W. Wen, G.C. Bazan, Post-deposition treatment of an arylated-carbazole conjugated polymer for solar cell fabrication, Adv. Mater. 24 (2012) 4505-4510, http://dx.doi.org/10.1002/adma.201201567.

[28] K. Zhang, Z. Hu, C. Duan, L. Ying, F. Huang, Y. Cao, The effect of methanol treatment on the performance of polymer solar cells, Nanotechnology 24 (2013) 484003, http://dx.doi.org/10.1088/0957-4484/24/48/484003.

[29] S. Nam, J. Jang, H. Cha, J. Hwang, T.K. An, S. Park, et al., Effects of direct solvent exposure on the nanoscale morphologies and electrical characteristics of PCBM-based transistors and photovoltaics, J. Mater. Chem. 22 (2012) 5543, http://dx.doi.org/10.1039/c2jm15260f.

[30] R.H. Bube, Photoconductivity of Solids, John Wiley & Sons Ltd, 1960.

[31] V.D. Mihailetchi, H. Xie, B. De Boer, L.J.A. Koster, P.W.M. Blom, Charge transport and photocurrent generation in poly(3-hexylthiophene): methanofullerene bulk-heterojunction solar cells, Adv. Funct. Mater. 16 (2006) 699-708, http://dx.doi.org/10.1002/adfm.200500420.

[32] A. Iacchetti, D. Natali, M. Binda, L. Beverina, M. Sampietro, Hopping photo- conductivity in an exponential density of states, Appl. Phys. Lett. 101 (2012) 103307, http://dx.doi.org/10.1063/1.4750239.

[33] F. Arca, S.F. Tedde, M. Sramek, J. Rauh, P. Lugli, O. Hayden, Interface trap states in organic photodiodes, Sci. Rep. 3 (2013) 1324, http://dx.doi.org/10.1038/srep01324.

[34] A. Teichler, J. Perelaer, U.S. Schubert, Inkjet printing of organic electronics e comparison of deposition techniques and state-of-the-art developments, J. Mater. Chem. C1 (2013) 1910, http://dx.doi.org/10.1039/c2tc00255h.

[35] B. Lim, J. Jo, S.-I. Na, J. Kim, S.-S. Kim, D.-Y. Kim, A morphology controller for high-efficiency bulk-heterojunction polymer solar cells, J. Mater. Chem. 20 (2010) 10919, http://dx.doi.org/10.1039/c0jm02296a.